Teleconnections between Tropical Pacific SST Anomalies and Extratropical Southern Hemisphere Climate

LAURA M. CIASTO

Climate Change Research Centre, University of New South Wales, Sydney, New South Wales, Australia, and Geophysical Institute, University of Bergen, and Bjerknes Centre for Climate Research, Bergen, Norway

GRAHAM R. SIMPKINS AND MATTHEW H. ENGLAND

Climate Change Research Centre, and ARC Centre of Excellence for Climate System Science, University of New South Wales, Sydney, New South Wales, Australia

(Manuscript received 20 June 2014, in final form 8 August 2014)

ABSTRACT

Teleconnections from tropical Pacific sea surface temperature (SST) anomalies to the high-latitude Southern Hemisphere (SH) are examined using observations and reanalysis. Analysis of tropical Pacific SST anomalies is conducted separately for the central Pacific (CP) and eastern Pacific (EP) regions. During the austral cold season, extratropical SH atmospheric Rossby wave train patterns are observed in association with both EP and CP SST variability. The primary difference between the patterns is the westward displacement of the CP-related atmospheric anomalies, consistent with the westward elongation of CP-related convective SST required for upper-level divergence and Rossby wave generation. Consequently, CP-related patterns of SH SST, Antarctic sea ice, and temperature anomalies also exhibit a westward displacement, but otherwise, the cold season extratropical SH teleconnections are largely similar. During the warm season, however, extratropical SH teleconnections associated with tropical CP and EP SST anomalies differ substantially. EP SST variability is linked to largely zonally symmetric structures in the extratropical atmospheric circulation, which projects onto the southern annular mode (SAM), and is strongly related to the SH temperature and sea ice fields. In contrast, CP SST variability is only weakly related to the SH atmospheric circulation, temperature, or sea ice fields and no longer exhibits any clear association with the SAM. One hypothesized mechanism suggests that the relatively weak CP-related SST anomalies are not able to substantially impact the background flow of the subtropical jet and its subsequent interaction with equatorward-propagating waves associated with variability in the SAM. However, there is currently no widely established mechanism that links tropical Pacific SST anomalies to the SAM.

1. Introduction

It has been widely established that extratropical Southern Hemisphere (SH) climate variability is strongly influenced by tropical Pacific sea surface temperature (SST) anomalies. In particular, SST variability centered in the tropical eastern Pacific, related to El Niño–Southern Oscillation (ENSO), is associated with large-scale changes in the extratropical SH atmospheric circulation (Karoly 1989; L'Heureux and Thompson 2006; Ding et al. 2012; Fogt et al. 2011), Southern Ocean SST anomalies (Ciasto and Thompson 2008; Ciasto and England 2011), Antarctic sea ice concentration anomalies (Liu et al. 2004; Simpkins et al. 2012), and Antarctic surface temperature anomalies (Kwok and Comiso 2002; Schneider et al. 2012).

Recent evidence indicates that the region of maximum tropical Pacific SST variability has shifted west toward the central Pacific since the 1990s (Ashok et al. 2007, 2009; Lee and McPhaden 2010; Xiang et al. 2013). For example, during the austral spring and summer of 2009/10, the central tropical Pacific experienced a warming that exceeded 5 times the standard deviation of SST anomalies in that region (Lee et al. 2010). It has been suggested that the increasing occurrence of central Pacific SST anomalies may be attributed to ongoing greenhouse gas warming (Ashok et al. 2007; Yeh et al. 2009). However, literature also shows that these

Corresponding author address: Laura M. Ciasto, Geophysical Institute, University of Bergen, Allégaten 70, 5007 Bergen, Norway. E-mail: laura.ciasto@gfi.uib.no

DOI: 10.1175/JCLI-D-14-00438.1

central Pacific SST anomalies may arise as the result of natural variability in ENSO (McPhaden et al. 2011; Newman et al. 2011). Given that there is no clear consensus on how the characteristics of tropical Pacific SST variability are expected to change over the coming century (Vecchi and Wittenberg 2010; Collins et al. 2010), it is important to understand the extent to which central Pacific SST variability impacts the global climate system.

Similar to their eastern Pacific counterparts, central Pacific SST anomalies also give rise to extratropical atmospheric teleconnections. A large fraction of the literature has focused on the global-scale teleconnections (e.g., Trenberth and Smith 2006), specific regions in the tropics (e.g., Taschetto et al. 2010; Hill et al. 2009; Chand et al. 2013), or the extratropical Northern Hemisphere (e.g., DiLorenzo et al. 2010; Yu and Kim 2011; Furtado et al. 2012; Ding et al. 2014). In contrast, relatively few studies have examined the extratropical SH teleconnections associated with central Pacific SST anomalies. Variability in the South Pacific SST and South American rainfall has been explored in relation to central Pacific SST variability (Li et al. 2013; Tedeschi et al. 2013). Lee et al. (2010) documented the impacts of the 2009/10 central Pacific SST warming event on the SH atmospheric circulation with implications for the Antarctic climate. Ding et al. (2011) further suggested that wintertime trends in Antarctic temperatures might be attributed to increased warming in the central Pacific. However, many aspects of the large-scale SH teleconnections associated with central Pacific SST variability have yet to be explored.

The objective of the current study is to provide a comparison of the large-scale extratropical SH atmospheric teleconnections associated with eastern and central tropical Pacific SST anomalies during both the austral cold and warm seasons. Teleconnections to the anomalous SH SST and Antarctic sea ice concentration and temperature fields are also explored, as they have not been quantified in relation to central Pacific SST variability, particularly in the austral warm season. The rest of this paper is outlined as follows: Section 2 provides a discussion of the data and methods used in the analysis. Sections 3 and 4 examine the relationships between tropical Pacific SST variability and several extratropical SH climate variables for the austral cold and warm seasons, respectively. Section 5 offers a discussion and summary of the key results of the study.

2. Data and methods

In this study, teleconnections to the SH high latitudes are compared using two contrasting regions of SST variability in the tropical Pacific: 1) eastern Pacific (EP) SST anomalies averaged over the area 10°N–10°S, 150°–90°W, coinciding with the Niño-3 region and 2) central Pacific (CP) SST anomalies averaged over the region 10°N–10°S, 150°E–160°W (Fig. 1, red boxes). The latter region overlaps some of the Niño-4 domain but is located west of the EP region to isolate SST variability between the central and eastern Pacific. While the two regions do not overlap, there is a positive correlation of 0.26 between the two SST anomaly time series, not statistically significant at the 95% level. Nonetheless, all analyses presented in this study were repeated using alternative conventional central and eastern Pacific SST indices, and all results obtained remain robust.

Monthly-mean SST and sea ice data are from the Hadley Centre Sea Ice and Sea Surface Temperature (HadISST) datasets (Rayner et al. 2003) and are derived using a blended analysis of in situ and satellite data. The 200-hPa wind divergence, 500-hPa geopotential height (Z_{500}), and 850-hPa winds are taken from the European Centre for Medium-Range Weather Forecasts (ECMWF) Interim Re-Analysis (ERA-Interim; Dee et al. 2011). Antarctic surface temperatures are taken from the Scientific Committee on Antarctic Research (SCAR) Reference Antarctic Data for Environmental Research (READER) database, a collection of meteorological observations from Antarctic research stations (Turner et al. 2004). The results presented here are not sensitive to the choice of reanalysis, SST, or sea ice products. Given that tropical teleconnections to the SH exhibit noticeable seasonal variations (Ciasto and Thompson 2008; Simpkins et al. 2012), the austral cold (July–September) and warm (November–February) seasons are analyzed separately. The results are not sensitive to the definition of the season. The analysis period is restricted to 1979–2011, when SH data are best constrained by satellite observations. Statistical significance of the correlation coefficients is assessed at the 95% confidence level using a two-tailed Student's t test (Bretherton et al. 1999).

3. Austral cold season

The top panel of Fig. 1 (shading) shows the austral cold season (June–September) Pacific SST anomalies regressed onto the standardized tropical EP (left) and CP (right) SST indices. Eastern tropical Pacific SST anomalies are dominated by warming (>1°C) that extends from South America to the date line. Central Pacific SST anomalies (Fig. 1, right), by contrast, exhibit strongest warming on the date line, with magnitudes that are substantially smaller (<0.5°C) than those observed in the eastern Pacific (Fig. 1, left). Despite the

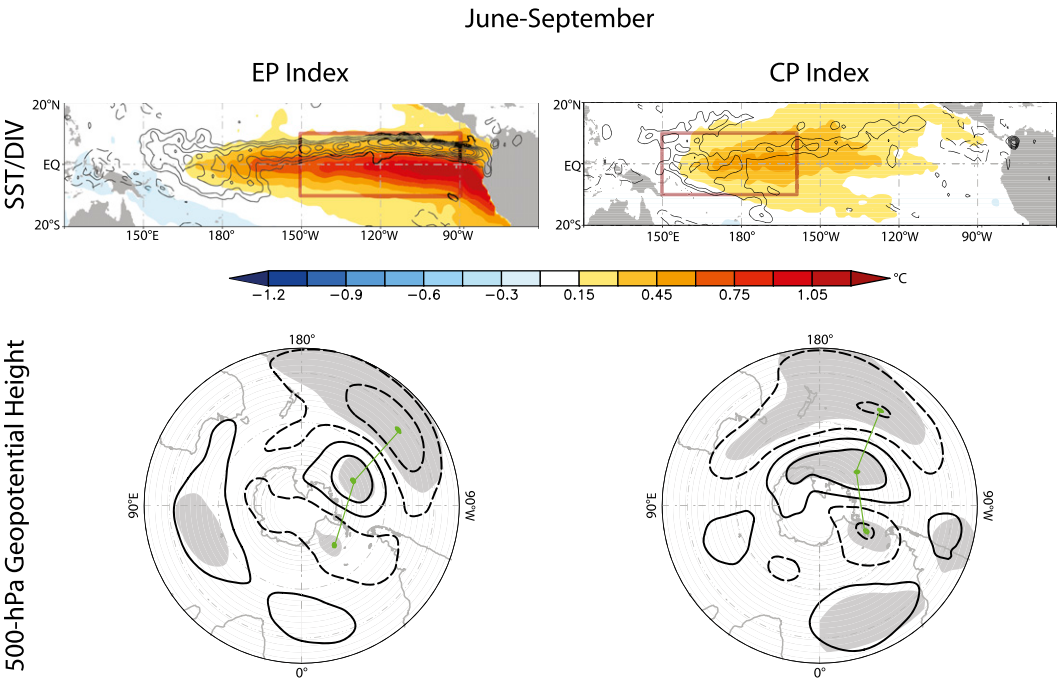

FIG. 1. Regressions of (top) SST (shading) and 200-hPa wind divergence (contours) and (bottom) Z_{500} anomalies (contours) onto the standardized (left) EP and (right) CP SST indices for the austral cold season (June–September). The red boxes correspond to the regions over which the EP and CP SST indices are averaged. Positive (negative) contours are denoted by solid (dashed) lines. The Z_{500} contours are drawn at intervals of 10 m, starting at ±15 m, and 200-hPa divergence contours are drawn at intervals of $2 \times 10^{-6}\,s^{-1}$, starting at $\pm 5 \times 10^{-6}\,s^{-1}$. Gray shading denotes Z_{500} regions exceeding the 95% confidence level based on a two-tailed Student's *t* test. The green dots represent the maximum amplitudes of the key centers of action and are connected with green lines.

differences in location and magnitude, both tropical CP and EP SST anomalies are associated with similar, and statistically significant, structures in the corresponding extratropical Z_{500} anomalies (Fig. 1, bottom), characterized by quasi-stationary Rossby waves. The most prominent difference between the teleconnection patterns is the overall westward displacement of the CP-related atmospheric anomalies relative to their EP counterpart (Fig. 1; cf. the location of green lines, connecting the centers of action of the Rossby wave trains).

The displacement of the SH Rossby wave train between tropical EP and CP SST anomalies is also reflected in the extratropical SH SST, Antarctic temperature, and sea ice concentration fields; however, as with the atmospheric circulation, the overall patterns display many similar features. As shown in Fig. 2 (top), both CP- and EP-related SH SST are marked by variability in the extratropical South Pacific and are consistent with turbulent heat fluxes and Ekman-related heat transport (not shown) associated with the low-level surface winds (Ciasto and Thompson 2008). The westward shift of the CP-related SH Rossby wave train also influences the structure of SST anomalies. Nevertheless, the magnitudes of the EP- and CP-related SST anomalies are comparable, except in the subtropical Pacific, where CP-related SST anomalies are weaker.

In the Antarctic region, sea ice concentration anomalies associated with both tropical CP and EP SST variability are dominated by a dipole between the Bellingshausen and Ross/Amundsen Seas (Fig. 2, bottom, shading). Such anomalies can be linked to heat fluxes and Ekman-induced ice advection related to the anticyclonic circulation over the Amundsen Sea (e.g., Liu et al. 2004). For example, warm northerlies in the western Amundsen Sea promote sea ice decline in that region. The converse is true in the presence of the cold southerlies in the Bellingshausen Sea, where sea ice growth is observed as well as decreasing surface air temperatures over the Antarctic Peninsula (Fig. 2, bottom, shaded circles). It is also observed that the anticyclonic circulation associated with the CP-related atmospheric circulation exhibits a more substantial westward elongation compared to the EP-related anticyclonic circulation. Consequently, the corresponding easterlies give rise to a more extensive pattern of decreasing sea ice concentration and increasing surface temperature anomalies around much of the Eastern Hemisphere.

The results in Figs. 1 and 2 reveal strong similarities between the EP and CP teleconnections despite the

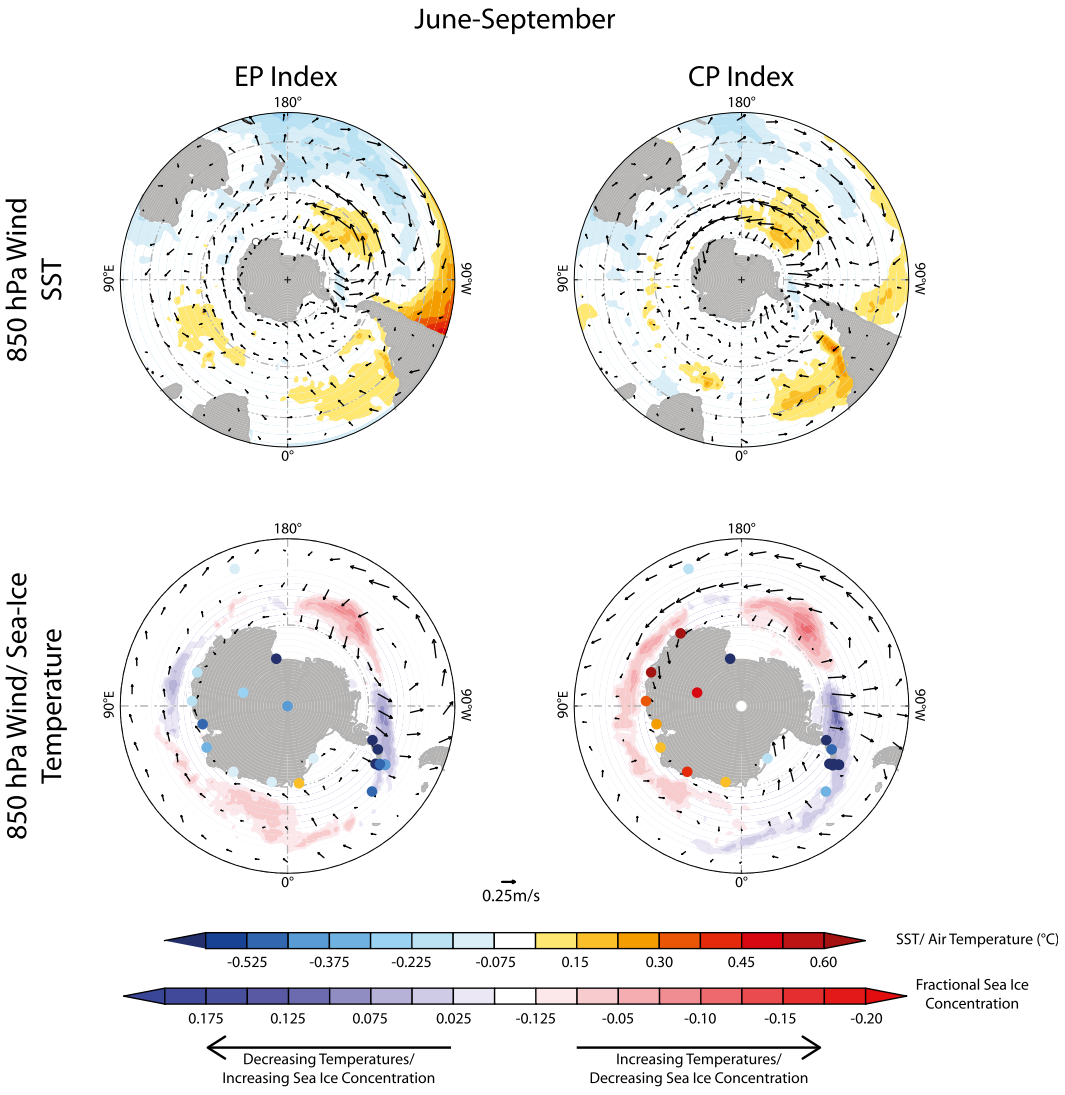

FIG. 2. Regressions of 850-hPa wind (arrows) with (top) SST (shading) and (bottom) surface temperature (filled circles) and sea ice concentration (shading) anomalies onto standardized (left) EP and (right) CP SST indices for the austral cold season (June–September). In (bottom), the focus is on the Antarctic region such that only wind vectors poleward of 50°S are shown.

considerable contrasts in the location and magnitude of the tropical EP and CP SST anomalies themselves. These similarities can be explained by comparing how the EP- and CP-related SST anomalies impact the convective SST field (i.e., total SST > 27.5°C). These convective SST changes are partly responsible for Rossby wave excitation: SST exceeding approximately 27.5°C gives rise to anomalous convective heating that is balanced by adiabatic cooling in ascent. The resulting upper-level divergence perturbations (Fig. 1, top, contours) are a key requirement for the generation of Rossby waves (e.g., Sardeshmukh and Hoskins 1988; Lachlan-Cope and Connolley 2006). The isotherms in Fig. 3 show the convective SST defined as the sum of the SST regression patterns in the top panel of Fig. 1 and the climatological-mean cold season SST. The eastern Pacific, where the CP and EP SST anomalies exhibit the strongest differences in magnitude (Fig. 3, shading), is not a region that is conducive for vertical motion (i.e., total SST do not exceed 27.5°C). Therefore, the large contrasts in anomalous SST magnitude in the eastern Pacific have little influence on the extratropical SH teleconnections. Rather the SH teleconnections are more influenced by the SST anomalies in the central/western Pacific, where much of the convective SST are observed. In these regions, the CP SST anomalies exceed the EP SST anomalies by approximately 0.3°C and are shifted westward. Consequently, the resulting maximum

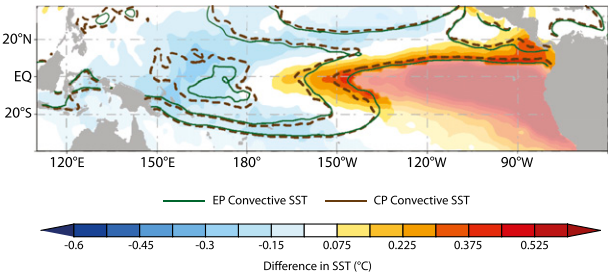

FIG. 3. Total SST associated with EP (green contours) and CP (brown dashed contours) SST indices for the austral cold (June–September) season. The total SST is defined as the sum of the SST regression patterns in the top panel of Fig. 1 and the climatological-mean cold season SST. Only total convective SST is shown such that contour intervals are drawn at 1.0°C intervals from 27.5°C. The shading corresponds to the difference in the CP- and EP-related total SST fields. Note that the CP/EP SST differences that lie outside of convective SST regions are transparently shaded.

CP-related divergence anomalies, a key source for Rossby wave excitation, are also observed farther west of the date line than the EP-related divergence anomalies (cf. the contours in the top panel of Fig. 1). The westward elongation of the maximum CP SST and attendant divergence anomalies may be a factor in the westward shift of the associated Rossby waves in the SH extratropics. Thus, the results presented in Figs. 1–3 indicate that austral cold season extratropical SH teleconnections are sensitive to the magnitude and location of tropical Pacific SST anomalies with respect to background SST. In particular, the projection of SST anomalies onto the climatological SST determines where maximum heating and vertical motion will occur.

4. Austral warm season

The structures of austral warm season CP and EP SST anomalies (Fig. 4, top, shading) are broadly similar to their cold season counterparts (Fig. 1). The largest difference is that warm season SST anomalies are stronger in magnitude than during the cold season, particularly those related to the CP index. However, a comparison of the warm season SH atmospheric circulation patterns associated with CP and EP indices (Fig. 4, bottom, contours) reveal more substantial differences than during the cold season. In particular, extratropical SH Z_{500} anomalies, which are significantly linked to EP SST variability, are only weakly linked to CP SST variability.

The extratropical SH atmospheric circulation associated with tropical EP SST anomalies is dominated by statistically significant positive height anomalies over the Amundsen Sea/Antarctica, surrounded by negative height anomalies (Fig. 4, bottom left). The zonally symmetric component of the structure projects onto the negative phase of the leading pattern of extratropical SH atmospheric variability, the southern annular mode (SAM). A correlation of −0.39 is observed between the SAM and EP SST index and is significant at the 95% confidence level. The relationship between the SAM

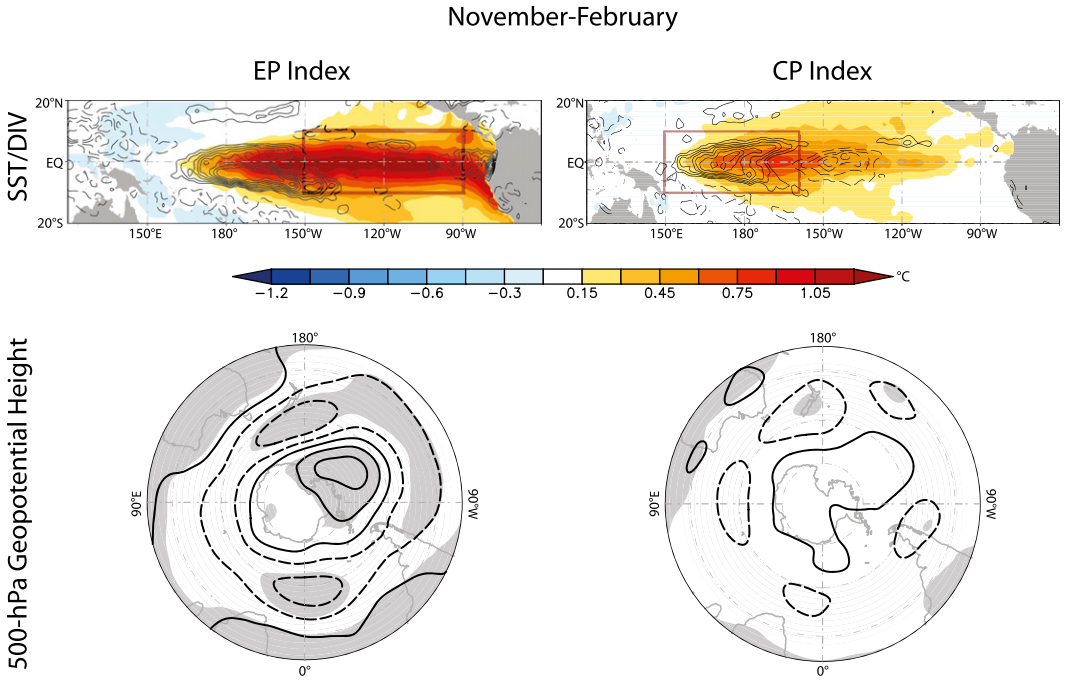

FIG. 4. As in Fig. 1, but regressions are now based on the austral warm season (November–February).

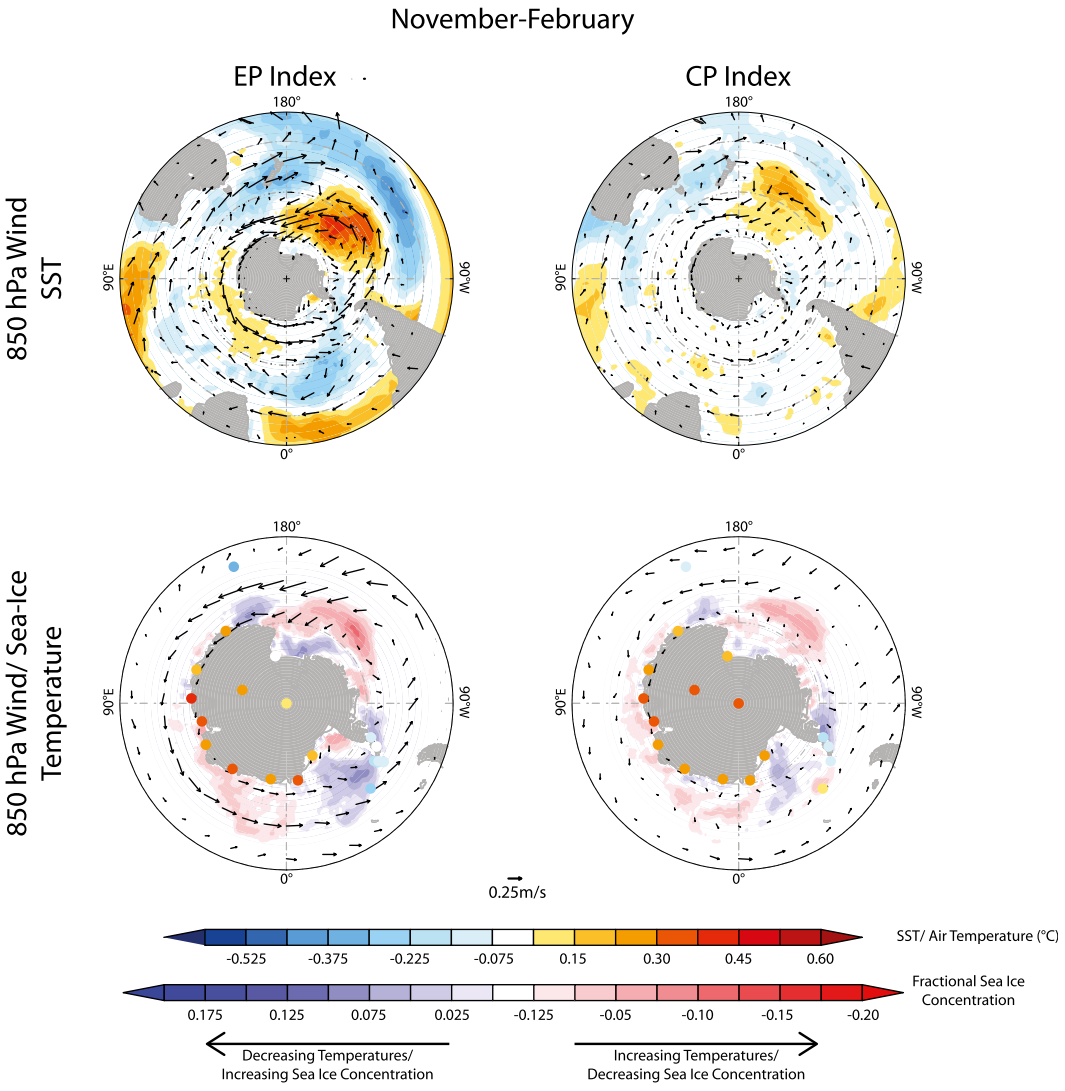

FIG. 5. As in Fig. 2, but regressions are now based on the austral warm season (November–February).

and eastern tropical Pacific SST anomalies has been established in several past studies, including L'Heureux and Thompson (2006) and Fogt et al. (2011). The pattern of EP-related Z_{500} anomalies in Fig. 4 also exhibits wavelike features that Ding et al. (2012) identified as a Rossby wave signature related to eastern tropical Pacific SST anomalies.

In contrast to EP-related teleconnections, extratropical SH atmospheric teleconnections associated with tropical CP SST variability are considerably weaker. The magnitudes of CP-related Z_{500} anomalies are less than half those associated with EP SST variability and only small, highly localized regions are significant at the 95% confidence level (Fig. 4, bottom right). While several centers of action still exist, this pattern of anomalous circulation projects weakly onto that of the SAM; the correlation between the SAM and CP SST indices during the warm season is −0.18, which fails to exceed the 95% significance level.

The large differences in the atmospheric circulation are further reflected in the underlying temperature and sea ice fields. The EP-related Z_{500} and low-level wind anomalies have considerable influence on the underlying temperature and sea ice fields (Fig. 5, left) through a combination of surface turbulent heat fluxes and meridional Ekman heat transport (not shown). In particular, the pattern of anomalous SH SST is marked by warming around much of the subtropics and cooling around 30°–50°S, except in the southeastern Pacific (90°–150°W), where positive anomalies are observed. The increasing temperature anomalies along the Antarctic coast are consistent with the overlying easterlies along 60°S. The anticyclonic circulation over the Amundsen Sea plays a key role in generating the dipole in Antarctic

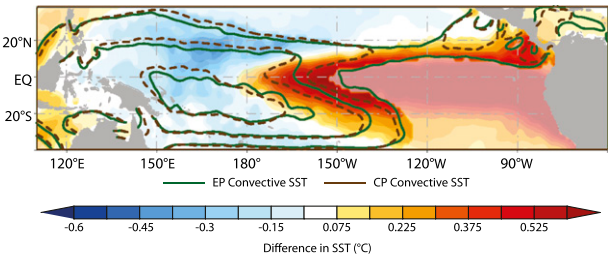

FIG. 6. As in Fig. 3, but results are now based on the austral warm season (November–February).

sea ice concentration anomalies through both meridional Ekman heat transport and turbulent heat fluxes. Overall, the patterns in Fig. 5 (left) are consistent with previous studies that have used other tropical eastern Pacific indices (e.g., Ciasto and England 2011; Simpkins et al. 2012).

In contrast to the statistically significant EP-related atmospheric circulation, the CP-related 850-hPa wind anomalies exhibit a less coherent structure of only modest amplitude (Fig. 5, right). As such, the attendant turbulent heat fluxes and Ekman heat transport have also weakened, which in turn impacts the magnitudes of the underlying anomalous temperature and sea ice fields. The pattern of SH SST anomalies associated with CP variability bears resemblance to its EP counterpart, but the magnitudes are considerably smaller. Over the Amundsen Sea, anticyclonic circulation anomalies are still evidenced in association with CP SST anomalies, but the attenuated amplitude gives rise to relatively modest changes in sea ice concentration, particularly around the Antarctic Peninsula.

The results above suggest that warm season SH teleconnections are sensitive to changes in the variability of tropical Pacific SST anomalies. However, diagnosing the extent to which the contrasting features of CP and EP SST variability account for the observed differences in the associated atmospheric teleconnections is difficult. There is no widely accepted mechanism to link tropical Pacific SST anomalies to the large-scale SH atmospheric circulation during this season. Although wavelike features are observed in both patterns of EP- and CP-related Z_{500} anomalies, the differences in the associated magnitudes cannot be solely explained by the differences in the tropical forcing of Rossby waves. If such forcing dominated the warm season tropical–extratropical interactions, the similarities between the EP and CP convective SST (Fig. 6), upper-level divergence (Fig. 4, top, contours) and inferred vertical motion would result in more similar Z_{500} circulation patterns than are observed in Fig. 4. Furthermore, Rossby wave propagation is thought to be inhibited during the austral warm season because of the poleward shift (~15°) and weakening of the subtropical jet, which thus becomes a less effective waveguide (Lee et al. 2009).

Several mechanisms have been postulated to explain the link between tropical Pacific SST and the zonally symmetric atmospheric circulation. One prevailing theory suggests that the SAM-related atmospheric circulation may be impacted by tropical SST anomalies through forcing of the background westerlies (i.e., subtropical jet) via thermal wind balance (e.g., L'Heureux and Thompson 2006). These altered background westerlies will, in turn, affect the critical latitudes of the equatorward-propagating waves associated with the SAM. For example, the meridional SST gradient associated with EP SST warming (Fig. 4) gives rise to upper-level subtropical westerlies (Fig. 7, left, shading) that, in turn, project onto the zonal background flow (Fig. 7, top left, contours). The resultant equatorward shift in the critical latitudes of the equatorward-propagating waves is consistent with the negative phase of the SAM. Following this hypothesis, CP-related SST anomalies, which are approximately 1.75 times weaker than their EP counterpart, result in a weaker impact on the subtropical background flow (Fig. 7, right) and thus do not strongly influence the critical latitude of the equatorward-propagating waves. As such, the relatively small CP-related anomalous meridional SST gradient is consistent with the reduced magnitude of the extratropical Z_{500} anomalies, which are roughly half the magnitude of their EP counterpart.

In the context of the mechanism proposed above, these results suggest that the difference in the maximum amplitude of EP- and CP-related SST anomalies might account for the observed differences in the associated teleconnections to the zonally symmetric extratropical atmospheric circulation. However, it remains uncertain which characteristics of the dissipation of the equatorward-propagating waves are most important: the *rate* of equatorward propagation (L'Heureux and Thompson 2006) or the *direction* of the wave propagation (Seager et al. 2003; Ceppi and Hartmann 2013). Gong et al. (2010) have also noted the dependency of the SAM-related wave breaking on the tropically forced changes in the background flow. They suggest that these changes are related to excitation of stratospheric SAM anomalies, which in turn influence the tropospheric variability.

Alternatively, it has been documented that variability in the latitude of the eddy-driven jet is significantly correlated to the latitudinal extent of the Hadley cell (Kang and Polvani 2011; Kidston et al. 2013). It is not clear to what extent these relationships are relevant for the link between variability in tropical SST and the SAM. The bottom panel of Fig. 7 (contours) shows the anomalous meridional streamfunction related to EP and

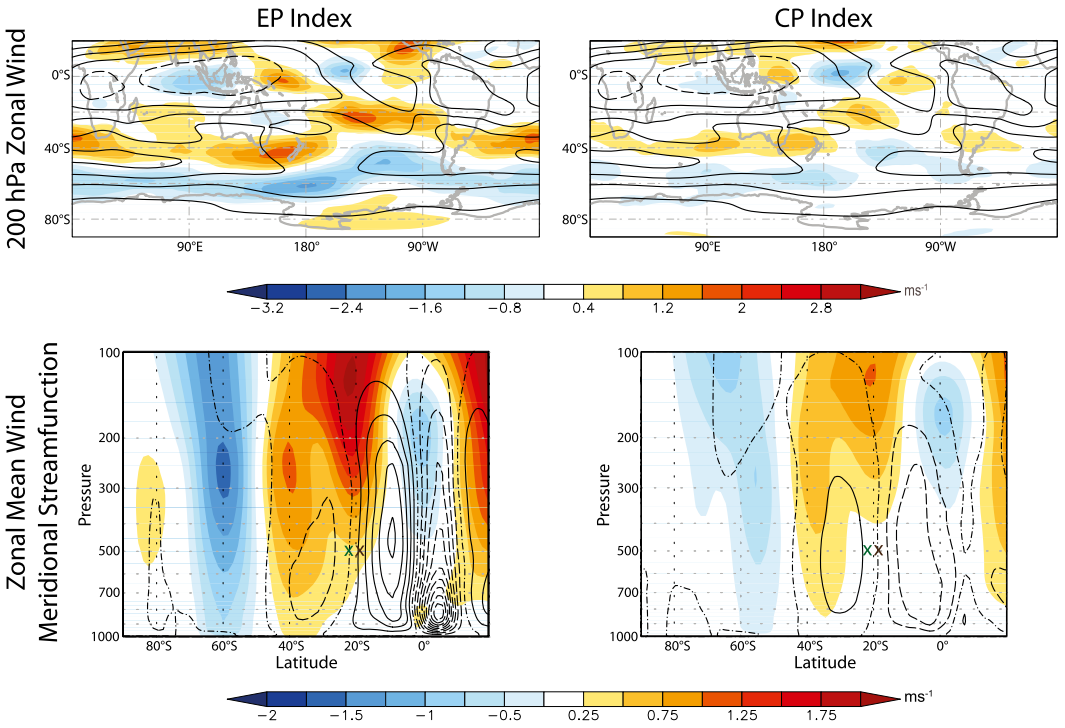

FIG. 7. Regressions of (top) 200-hPa zonal wind (shading) and (bottom) zonal-mean wind (shading) and meridional streamfunction (contours) anomalies onto the standardized (left) EP and (right) CP SST indices for the austral warm season (November–February). In (top), climatological-mean 200-hPa zonal wind positive (negative) contours are denoted by solid (dashed) lines and are drawn at intervals of 10 m s^{-1}. In (bottom), counterclockwise (clockwise) motion corresponds to solid (dashed) contours and is drawn at intervals of 1.5×10^9 kg s^{-1}. Crosses denote the EP-related (green) and CP-related (brown) latitudinal extent of the Hadley cell.

CP SST anomalies. The Hadley cell extent is defined as the latitude of the first zero crossing (moving poleward from the tropical circulation) of the meridional streamfunction at 500 hPa. A slight poleward shift of CP-related Hadley circulation (brown cross) is observed in comparison to its EP counterpart (green cross). Nevertheless, the weaker CP-related Hadley circulation also suggests that CP SST anomalies are simply not strong enough to perturb the extratropical SH atmospheric circulation.

5. Summary

The objective of this study is to compare the patterns of extratropical SH atmosphere–ocean–sea ice variability in relation to contrasting patterns of tropical SST variability in the eastern and central Pacific. While several studies have documented the SH atmospheric circulation associated with various patterns of tropical SST variability, the present analysis further examines the Southern Ocean SST, Antarctic surface air temperature, and sea ice concentration anomalies in the cold season (June–September) and previously undocumented warm season (November–April).

During the austral cold season, the SH teleconnections associated with EP and CP SST variability exhibit strong similarities in terms of their magnitudes and structures. Rossby wave train structures are observed in association with both regions with only a shifting of the centers of action (Fig. 1). As such, the resulting differences between the patterns of SH SST, Antarctic temperature and sea ice fields are also modest (Fig. 2). The primary exception is in the east Antarctic region where changes in the anomalous atmospheric circulation over the Amundsen Sea have significant implications for the underlying temperature and sea ice fields. The results suggest that the comparison of the atmospheric teleconnection patterns is consistent with the location and magnitude of the tropical Pacific SST west of the date line. In particular, it is how the SST anomalies project onto the convectively primed climatological SST (Fig. 3) that partly determines the magnitude and structure of the resulting Rossby waves, consistent with previous studies (Lachlan-Cope and Connolley 2006).

During the austral warm season, the similarities between SH teleconnections associated with EP and CP

SST variability are considerably weaker (Fig. 4). The pattern of Z_{500} anomalies associated with the EP SST variability projects strongly onto the leading mode of extratropical atmospheric variability, the SAM. In turn, this SAM-like signature in the SH atmospheric circulation has significant impacts on the underlying SH climate as shown in Fig. 5 and is consistent with previous studies using other eastern Pacific SST indices. However, teleconnections between the CP SST variability and the extratropical SH Z_{500} anomalies are relatively weak, thus having only a modest impact on the underlying temperature and sea ice fields (Fig. 5). Unlike the austral cold season, it is unclear to what extent the differences in the location and magnitude of the CP and EP SST variability account for the differences in the associated SH teleconnections. Within the context of the hypotheses that place importance on changes in the subtropical jet, the weak CP SST anomalies relative to the EP anomalies is a key factor accounting for the different teleconnection patterns. However, other hypotheses place importance on stratospheric wave breaking or the latitudinal shifts in the edge of the Hadley cell.

The analysis presented here focuses on extratropical SH teleconnections associated with two regions in the tropical Pacific that are not entirely unrelated. As shown in section 2, they exhibit a positive (but nonsignificant) correlation of 0.26. Thus it should be considered whether comparisons of EP- and CP-related teleconnection patterns merely reflect the extension of SST variability across both regions, rather than distinct signatures of EP and CP SST variability. Composite analyses were calculated such that the maximum warming is focused in only one of these regions. The results (not shown) demonstrate that the analyses are qualitatively similar to those based on the regressions presented here. In particular, teleconnections to the SH high latitudes weaken considerably for CP SST anomalies during the warm season. Furthermore, the lead–lag relationships between the atmospheric circulation and tropical SST have also been examined with no detection of significant relationships beyond the zero lag in the warm or cold seasons. These results suggest that neither the contemporaneous nor lagged relationships between the CP and EP SST variability can explain the observed differences presented here.

The results of this study suggest that the effect of location and magnitude of tropical SST variability on the extratropical teleconnections varies between seasons. Cold season SH teleconnection patterns appear to be influenced most strongly by the location and magnitude of the convective SST while warm season SH teleconnections appear more sensitive to the magnitude of the SST anomalies themselves. However, this study is by no means a comprehensive examination of the factors involved in tropical–extratropical interactions. Indeed, numerical experiments are likely essential to diagnose the physical mechanism behind the relative importance of magnitude and location of tropical Pacific SST anomalies for SH teleconnections. This study presents an observational analysis focusing on the identification of the variations in the SH teleconnections originating from tropical Pacific variability. Regardless of the underlying mechanisms driving these relationships, the results shown here demonstrate that the SH climate is strongly impacted by changes in the patterns of tropical SST variability. Documenting the impact of tropical Pacific SST variability on extratropical climate is crucial given that it is uncertain how characteristics of the tropical climate will evolve under future climate change.

Acknowledgments. We thank Drs. Andrea Taschetto, Shayne McGregor, and Justin Wettstein for useful discussions of the results. This research was supported by the Australian Research Council.

REFERENCES

Ashok, K., S. K. Behera, S. A. Rao, H. Weng, and T. Yamagata, 2007: El Niño Modoki and its possible teleconnection. *J. Geophys. Res.,* **112,** C11007, doi:10.1029/2006JC003798.

——, C.-Y. Tam, and W.-J. Lee, 2009: ENSO Modoki impact on the Southern Hemisphere storm track activity during extended austral winter. *Geophys. Res. Lett.,* **36,** L12705, doi:10.1029/2009GL038847.

Bretherton, C. S., M. Widmann, V. P. Dymnikov, J. M. Wallace, and I. Blade, 1999: Effective number of degrees of freedom of a spatial field. *J. Climate,* **12,** 1990–2009, doi:10.1175/1520-0442(1999)012<1990:TENOSD>2.0.CO;2.

Ceppi, P., and D. L. Hartmann, 2013: On the speed of the eddy-driven jet and the width of the Hadley cell. *J. Climate,* **26,** 3450–3465, doi:10.1175/JCLI-D-12-00414.1.

Chand, S. S., J. L. McBride, K. J. Tory, M. C. Wheeler, and K. J. E. Walsh, 2013: Impact of different ENSO regimes on southwest Pacific tropical cyclones. *J. Climate,* **26,** 600–608, doi:10.1175/JCLI-D-12-00114.1.

Ciasto, L. M., and D. W. J. Thompson, 2008: Observations of large-scale ocean–atmosphere interaction in the Southern Hemisphere. *J. Climate,* **21,** 1244–1259, doi:10.1175/2007JCLI1809.1.

——, and M. H. England, 2011: Observed ENSO teleconnections to Southern Ocean SST anomalies diagnosed from a surface mixed layer heat budget. *Geophys. Res. Lett.,* **38,** L09701, doi:10.1029/2011GL046895.

Collins, M., and Coauthors, 2010: The impact of global warming on the tropical Pacific Ocean and El Niño. *Nat. Geosci.,* **3,** 391–397, doi:10.1038/ngeo868.

Dee, D. P., and Coauthors, 2011: The ERA-Interim reanalysis: Configuration and performance of the data assimilation system. *Quart. J. Roy. Meteor. Soc.,* **137,** 553–597, doi:10.1002/qj.828.

Di Lorenzo, E., K. M. Cobb, J. C. Furtado, N. Schneider, B. T. Anderson, A. Bracco, M. A. Alexander, and D. J. Vimont, 2010: Central Pacific El Niño and decadal climate change in the North Pacific. *Nat. Geosci.,* **3,** 762–765, doi:10.1038/ngeo984.

Ding, Q., E. J. Steig, D. S. Battisti, and M. Kuettel, 2011: Winter warming in West Antarctica caused by central tropical Pacific warming. *Nat. Geosci.,* **4,** 398–403, doi:10.1038/ngeo1129.

——, ——, ——, and J. M. Wallace, 2012: Influence of the tropics on the southern annular mode. *J. Climate,* **25,** 6330–6348, doi:10.1175/JCLI-D-11-00523.1.

——, J. M. Wallace, D. S. Battisti, E. J. Steig, A. E. J. Gallant, H. J. Kim, and L. Geng, 2014: Tropical forcing of the recent rapid Arctic warming in northeastern and Greenland. *Nature,* **509,** 209–212, doi:10.1038/nature13260.

Fogt, R. L., D. H. Bromwich, and K. M. Hines, 2011: Understanding the SAM influence on the South Pacific ENSO teleconnection. *Climate Dyn.,* **36,** 1555–1576, doi:10.1007/s00382-010-0905-0.

Furtado, J. C., E. Di Lorenzo, B. T. Anderson, and N. Schneider, 2012: Linkages between the North Pacific Oscillation and central tropical Pacific SSTs at low frequencies. *Climate Dyn.,* **39,** 2833–2846, doi:10.1007/s00382-011-1245-4.

Gong, T., S. B. Feldstein, and D. Luo, 2010: The impact of ENSO on wave breaking and southern annular mode events. *J. Atmos. Sci.,* **67,** 2854–2870, doi:10.1175/2010JAS3311.1.

Hill, K. J., A. S. Taschetto, and M. H. England, 2009: South American rainfall impacts associated with inter-El Niño variations. *Geophys. Res. Lett.,* **36,** L19702, doi:10.1029/2009GL040164.

Kang, S. M., and L. M. Polvani, 2011: The interannual relationship between the latitude of the eddy-driven jet and the edge of the Hadley cell. *J. Climate,* **24,** 563–568, doi:10.1175/2010JCLI4077.1.

Karoly, D. J., 1989: Southern Hemisphere circulation features associated with El Niño-Southern Oscillation events. *J. Climate,* **2,** 1239–1252, doi:10.1175/1520-0442(1989)002<1239:SHCFAW>2.0.CO;2.

Kidston, J., C. W. Cairns, and P. Paga, 2013: Variability in the width of the tropics and the annular modes. *Geophys. Res. Lett.,* **40,** 2328–2332, doi:10.1029/2012GL054165.

Kwok, R., and J. C. Comiso, 2002: Spatial patterns of variability in Antarctic surface temperature: Connections to the South Hemisphere annular mode and the Southern Oscillation. *Geophys. Res. Lett.,* **29,** 1705, doi:10.1029/2002GL015415.

Lachlan-Cope, T., and W. Connolley, 2006: Teleconnections between the tropical Pacific and the Amundsen-Bellinghausens Sea: Role of the El Niño/Southern Oscillation. *J. Geophys. Res.,* **111,** D23101, doi:10.1029/2005JD006386.

Lee, S.-K., C. Wang, and B. E. Mapes, 2009: A simple atmospheric model of the local and teleconnection responses to tropical heating anomalies. *J. Climate,* **22,** 272–284, doi:10.1175/2008JCLI2303.1.

Lee, T., and M. J. McPhaden, 2010: Increasing activity of El Niño in the central-equatorial Pacific. *Geophys. Res. Lett.,* **37,** L14603, doi:10.1029/2010GL044007.

——, and Coauthors, 2010: Record warming in the South Pacific and western Antarctica associated with the strong central-Pacific El Niño in 2009–10. *Geophys. Res. Lett.,* **37,** L19704, doi:10.1029/2010GL044865.

L'Heureux, M. L., and D. W. J. Thompson, 2006: Observed relationships between the El Niño–Southern Oscillation and the extratropical zonal-mean circulation. *J. Climate,* **19,** 276–287, doi:10.1175/JCLI3617.1.

Li, G., C. Y. Li, Y. K. Tan, and J. Pan, 2013: Impacts of the central and eastern Pacific types of ENSO on sea surface temperature in the South Pacific. *Theor. Appl. Climatol.,* **114,** 315–327, doi:10.1007/s00704-013-0840-1.

Liu, J., J. A. Curry, and D. G. Martinson, 2004: Interpretation of recent Antarctic sea ice variability. *Geophys. Res. Lett.*, **31,** L02205, doi:10.1029/2003GL018732.

McPhaden, M. J., T. Lee, and D. McClurg, 2011: El Niño and its relationship to changing background conditions in the tropical Pacific Ocean. *Geophys. Res. Lett.,* **38,** L15709, doi:10.1029/2011GL048275.

Newman, M., S.-I. Shin, and M. A. Alexander, 2011: Natural variation in ENSO flavors. *Geophys. Res. Lett.,* **38,** L14705, doi:10.1029/2011GL047658.

Rayner, N. A., D. E. Parker, E. B. Horton, C. K. Folland, L. V. Alexander, D. P. Rowell, E. C. Kent, and A. Kaplan, 2003: Global analyses of sea surface temperature, sea ice, and night marine air temperature since the late nineteenth century. *J. Geophys. Res.,* **108,** 4407, doi:10.1029/2002JD002670.

Sardeshmukh, P. D., and B. J. Hoskins, 1988: The generation of global rotational flow by steady idealized tropical divergence. *J. Atmos. Sci.,* **45,** 1228–1251, doi:10.1175/1520-0469(1988)045<1228:TGOGRF>2.0.CO;2.

Schneider, D. P., Y. Okumura, and C. Deser, 2012: Observed Antarctic climate variability and tropical linkages. *J. Climate,* **25,** 4048–4066, doi:10.1175/JCLI-D-11-00273.1.

Seager, R., N. Harnik, Y. Kushnir, W. Robinson, and J. Miller, 2003: Mechanisms of hemispherically symmetric climate variability. *J. Climate,* **16,** 2960–2978, doi:10.1175/1520-0442(2003)016<2960:MOHSCV>2.0.CO;2.

Simpkins, G. R., L. M. Ciasto, D. W. J. Thompson, and M. H. England, 2012: Seasonal relationships between large-scale climate variability and Antarctic sea ice concentration. *J. Climate,* **25,** 5451–5469, doi:10.1175/JCLI-D-11-00367.1.

Taschetto, A. S., R. J. Haarsma, A. Sen Gupta, C. C. Ummenhofer, K. J. Hill, and M. H. England, 2010: Australian monsoon variability driven by a Gill–Matsuno-type response to central west Pacific warming. *J. Climate,* **23,** 4717–4736, doi:10.1175/2010JCLI3474.1.

Tedeschi, R. G., I. F. A. Cavalcanti, and A. M. Grimm, 2013: Influences of two types of ENSO on South American precipitation. *Int. J. Climatol.,* **33,** 1382–1400, doi:10.1002/joc.3519.

Trenberth, K. E., and L. Smith, 2006: The vertical structure of temperature in the tropics: Different flavors of El Niño. *J. Climate,* **19,** 4956–4973, doi:10.1175/JCLI3891.1.

Turner, J., and Coauthors, 2004: The SCAR READER project: Toward a high-quality database of mean Antarctic meteorological observations. *J. Climate,* **17,** 2890–2898, doi:10.1175/1520-0442(2004)017<2890:TSRPTA>2.0.CO;2.

Vecchi, G. A., and A. T. Wittenberg, 2010: El Niño and our future climate: Where do we stand? *Wiley Interdiscip. Rev.: Climate Change,* **1,** 260–270, doi:10.1002/wcc.33.

Xiang, B., B. Wang, and T. Li, 2013: A new paradigm for the predominance of standing central Pacific warming after the late 1990s. *Climate Dyn.,* **41,** 327–340, doi:10.1007/s00382-012-1427-8.

Yeh, S. W., J. S. Kug, B. Dewitte, M. H. Kwon, B. P. Kirtman, and F. F. Jin, 2009: El Niño in a changing climate. *Nature,* **461,** 511–514, doi:10.1038/nature08316.

Yu, J.-Y., and S. T. Kim, 2011: Relationships between extratropical sea level pressure variations and the central Pacific and eastern Pacific types of ENSO. *J. Climate,* **24,** 708–720, doi:10.1175/2010JCLI3688.1.